

A New Non-Abelian Topological Phase of Cold Fermi Gases in Anisotropic and Spin-Dependent Optical Lattices

Beibing Huang *

Department of Experiment Teaching, Yancheng Institute of Technology, Yancheng, 224051, China

Xiaosen Yang and ShaoLong Wan

Institute for Theoretical Physics and Department of Modern Physics
University of Science and Technology of China, Hefei, 230026, China

June 1, 2018

Abstract

To realize non-Abelian s-wave topological superfluid of cold Fermi gases, generally a Zeeman magnetic field larger than superfluid pairing gap is necessary. In this paper we find that using an anisotropic and spin-dependent optical lattice to trap gases, a new non-Abelian topological superfluid phase appears, in contrast to an isotropic and spin-independent optical lattice. A characteristic of this new non-Abelian topological superfluid is that Zeeman magnetic field can be smaller than the superfluid pairing gap. By self-consistently solving pairing gap equation and considering the competition against normal state and phase separation, this new phase is also stable. Thus an anisotropic and spin-dependent optical lattice supplies a convenient route to realize topological superfluid. We also investigate edge states and the effects of a harmonic trap potential.

PACS number(s): 67.85.Lm, 03.65.Vf, 74.20.-z

1 Introduction

In two dimensional condensed matter physics, the search of non-Abelian Majorana fermions (MF) [1], which are their own antiparticles and may have potential important application

*Corresponding author. Electronic address: hbb4236@mail.ustc.edu.cn

in fault-tolerant topological quantum computation [2], attracts much recent attention to topological superfluid (TS) and superconductors (TSC) [3, 4], which has a full pairing gap in the bulk and topologically protected gapless states on the boundary. Inspired by the fact that MFs exist at the vortex cores of a two-dimensional (2D) $p_x + ip_y$ superconductor [5], theoretically some practical systems have been proposed, such as fractional quantum Hall effect at filling $\nu = 5/2$ [5], superfluid He-3 [6], non-centrosymmetric superconductors [7, 8], the surface of a three-dimensional topological insulator in proximity to an s-wave superconductor [9, 10] and a spin-orbit-coupled (SOC) semiconductor quantum well coupled to an s-wave superconductivity and a ferromagnetic insulator [11]. Especially the latter has been improved by applying an in-plane magnetic field to a (110)-grown semiconductor coupled only to an s-wave superconductor. This improvement not only enhances the ability to tune into the topological superconducting state but also avoid orbital effect of the external magnetic field [12].

It is widely known that cold Fermi gases can be used to simulate many other systems owing to their many controllable advantages and operabilities. Certainly the simulations to TS are also possible and as far as what we know is concerned, three main routes have been suggested. The first was direct and based on p-wave superfluidity of degenerate Fermi gases by means of p-wave Feshbach resonance [13]. Although this method is very simple, it is challenging due to short lifetimes of the p-wave pairs and molecules. Subsequently Zhang et al. [14] propose to create an effective $p_x + ip_y$ TS from an s-wave interaction making use of an artificially generated SOC. In fact, SOC have been realized in a neutral atomic Bose-Einstein condensate (BEC) and the same technique is also feasible for cold Fermi gases [15, 16]. Realizing that in a dual transformation SOC is formally equivalent to a p-wave superfluid gap, Sato et al. [17] suggest to artificially generate the vortices of SOC by using lasers carrying orbital angular momentum. In terms of the latter two ansatzs, in order to enter into non-Abelian TS, a Zeeman magnetic field larger than superfluid pairing gap is essentially needed.

In this paper we propose a model to realize non-Abelian TS in cold Fermi gases by using an anisotropic and spin-dependent optical lattice (ASDOL) to engineer mismatched Fermi surfaces for each hyperfine species. Such two requirements for optical lattices are both accessible in an experiment. The anisotropy is determined by the intensity of the corresponding pair of laser beams in different directions, while spin-dependence is also available in the light of the fact that the strength of the optical potential crucially depends on the atomic dipole moment between the internal states involved [18, 19, 20, 21]. In contrast to an isotropic and spin-independent optical lattice (ISIOL) [14, 17], our model realizes another new non-Abelian TS phase in which Zeeman magnetic field can be smaller than superfluid pairing gap.

The organization of this paper is as follows. In section 2, we firstly give our model and analyze the condition of gap closing. Then we calculate TKNN number I_{TKNN} [22] of occupied bands addressing the topological properties of the model to obtain topological phase diagram. A new non-Abelian TS is discovered. In addition we also investigate the properties of edge states to prove bulk-boundary correspondence. In section 3, by taking the self-consistency constraint on the s-wave pairing gap into account, the stability of TS and the effects of a harmonic trap potential are discussed. We find that this new non-Abelian TS is stable. A brief conclusion is given in Section 4.

2 Hamiltonian and Topological Phase Diagram

In this paper we consider s-wave superfluid of cold Fermi gases with Rashba SOC in a two-dimension square optical lattice which is anisotropic and spin-dependent. For convenience below we assume the lattice constant to be unit. The Hamiltonian suggested is

$$H = \sum_{k\sigma} [\epsilon_{k\sigma} - \mu - \sigma\Gamma] a_{k\sigma}^\dagger a_{k\sigma} + \sum_k [J_k a_{k\uparrow}^\dagger a_{k\downarrow} - \Delta a_{-k\downarrow} a_{k\uparrow} + H.C.], \quad (1)$$

where $a_{k\sigma}^\dagger$ creates a spin $\sigma = \uparrow, \downarrow$ fermion at momentum $\vec{k} = (k_x, k_y)$. $J_k = 2J[\sin(k_y) + i \sin(k_x)]$ with J ($J > 0$) denoting the strength of Rashba SOC. μ , Γ , Δ are chemical potential, effective Zeeman magnetic field and s-wave superfluid pairing gap, respectively.

The kinetic energy terms $\epsilon_{k\sigma}$ come from anisotropic and spin-dependent optical lattices [23]. Imagine tuning the intensities of lasers so that one spin state prefers to hop along the x axis and the other prefers to hop along the y axis. In this paper we concentrate on a specific situation where the Fermi surfaces of the two spin states are rotated by 90° with respect to one another, and only consider a near-neighbor hopping Hamiltonian with single particle dispersions

$$\begin{aligned} \epsilon_{k\uparrow} &= -2t_a \cos(k_x) - 2t_b \cos(k_y), \\ \epsilon_{k\downarrow} &= -2t_b \cos(k_x) - 2t_a \cos(k_y). \end{aligned} \quad (2)$$

When there are no Zeeman magnetic field and SOC $\Gamma = J = 0$, this model realized a stable paired superfluid state with coexisting pockets of momentum space with gapless unpaired fermions [23], similar to the Sarma state in polarized mixtures [24, 25, 26]. Moreover in the strong coupling limit, a d-wave pairing superfluid as well as a d-wave density wave state, are also proposed to be achievable in this system [27].

Generally speaking, the close of bulk gap is a signal of topological phase transitions, although it is not a sufficient condition [28]. Thus to obtain topological phase diagram of Hamiltonian (1), we firstly calculate the bulk spectrum of the system to search parameter regions for which different topological phases are possible. Then for every regions we calculate topological invariants to label topological properties. To obtain the bulk spectrum, we rewrite the Hamiltonian as

$$H = \frac{1}{2} \sum_k \psi_k^\dagger M_{4 \times 4} \psi_k, \quad (3)$$

where $\psi_k^\dagger = (a_{k\uparrow}^\dagger, a_{k\downarrow}^\dagger, a_{-k\uparrow}, a_{-k\downarrow})$ is a row vector and $M_{4 \times 4}$ is a matrix with $M_{11} = -M_{33} = \epsilon_{k\uparrow} - \mu - \Gamma$, $M_{22} = -M_{44} = \epsilon_{k\downarrow} - \mu + \Gamma$, $M_{12} = M_{43} = M_{21}^* = M_{34}^* = J_k$, $M_{23} = M_{32} = -M_{14} = -M_{41} = \Delta$, $M_{13} = M_{31} = M_{24} = M_{42} = 0$.

Diagonalizing the matrix $M_{4 \times 4}$, we find the energy spectrum

$$E_k^\pm = \sqrt{\xi_{k+}^2 + \xi_{k-}^2 + |J_k|^2 + \Delta^2} \pm 2E_0 \quad (4)$$

with $\xi_{k+} = -(t_a + t_b)[\cos(k_x) + \cos(k_y)] - \mu$, $\xi_{k-} = (-t_a + t_b)[\cos(k_x) - \cos(k_y)] - \Gamma$ and $E_0 = \sqrt{\xi_{k+}^2 \xi_{k-}^2 + \xi_{k+}^2 |J_k|^2 + \xi_{k-}^2 \Delta^2}$.

The close of the bulk energy gap is possible only if $E_k^- = 0$, in other words

$$\xi_{k+}^2 + \xi_{k-}^2 + |J_k|^2 + \Delta^2 = 2E_0, \quad (5)$$

which is equivalent to

$$\xi_{k+}^2 - \xi_{k-}^2 - |J_k|^2 + \Delta^2 = 0, \quad |J_k|^2 \Delta^2 = 0. \quad (6)$$

For the s-wave pairing, $\Delta \neq 0$ and the second equation in (6) is satisfied only when $k = (0, 0), (0, \pi), (\pi, 0), (\pi, \pi)$. Substituting these values into the first equation in (6), four different gap closing conditions are obtained

$$\begin{aligned} \mu^2 + \Delta^2 &= [2(t_b - t_a) + \Gamma]^2, & \mu^2 + \Delta^2 &= [2(t_b - t_a) - \Gamma]^2, \\ \Gamma^2 &= \Delta^2 + [2(t_a + t_b) + \mu]^2, & \Gamma^2 &= \Delta^2 + [2(t_a + t_b) - \mu]^2. \end{aligned} \quad (7)$$

By means of these conditions, Fig.1(a) shows that there are at least 12 regions, which may be topologically distinct. By now we have completed the first step of deciding topological phase diagram. Below we will explore the topological numbers to classify the topological phases of the model (1).

In terms of our system, it explicitly breaks the time-reversal symmetry even though Zeeman magnetic field is zero. Thus TKNN number I_{TKNN} plays a central role in topological nature of the system [22], which is consistent with the conclusion in the periodic table of TSC that BdG Hamiltonian only with particle-hole symmetry in two dimension is classified by integer group Z [29]. Furthermore the topological properties of the system are identified as follows [30]. If TKNN number is nonzero and even (odd), the system is Abelian (non-Abelian) TS without (with) non-Abelian anyons; If TKNN number is zero, the system is topologically trivial and is normal superfluid.

TKNN number is defined by

$$I_{TKNN} = \frac{1}{2\pi i} \int d^2k F_{12}(k), \quad (8)$$

where Berry connection $A_i(k)$ ($i = 1, 2$) and associated field strength $F_{12}(k)$ are given by

$$\begin{aligned} A_i(k) &= \sum_{E_n < 0} \langle \phi_n(k) | \partial_{k_i} \phi_n(k) \rangle \\ F_{12}(k) &= \partial_1 A_2(k) - \partial_2 A_1(k) \end{aligned} \quad (9)$$

with $|\phi_n(k)\rangle$ being a normalized wave function of the n th band such that $M_{4 \times 4} |\phi_n(k)\rangle = E_n(k) |\phi_n(k)\rangle$. It should be noted that the sum in (9) is restricted to occupied bands.

TKNN numbers of 12 regions have been numerically calculated [31] and given in Fig.1(a). Totally 5 non-Abelian TS and one Abelian TS phases are found. In order to make a contrast, in Fig.1(b) we also show the topological phase diagram of an ISIOI and there are 4 non-Abelian TS and 1 Abelian TS phases. By comparison the effects of ASDOL are mainly twofolds. On the one hand it creates another non-Abelian TS phase around the chemical potential $\mu = 0$, which can be realized for Zeeman magnetic field Γ less than superfluid pairing gap Δ . This is our main result in this paper and can be understood from the fact that an ASDOL ($t_a \neq t_b$) supplies an effective Zeeman magnetic field $\pm 2(t_a - t_b)$, as

seen from (7). On the other hand in the direction of increasing Zeeman magnetic field it separates two successive non-Abelian TS phases in Fig.1(b).

According to the bulk-boundary correspondence, a topologically nontrivial bulk guarantees the existence of topologically stable gapless edge states on the boundary. Cold Fermi gases with sharp edges may be realized along the lines proposed in [32]. In our case, the gapless edge states is a chiral Majorana fermion mode. It should also be remembered that the core of a vortex is topologically equivalent to an edge which has been closed on itself. The topologically protected edge modes we describe here are therefore equivalent to the Majorana fermions known to exist in the core of vortices of p-wave superfluid [33].

To study edge states, we transform Hamiltonian (1) into lattice representation

$$\begin{aligned}
H = & -t_a \sum_i [a_{i\uparrow}^\dagger a_{i+x\uparrow} + a_{i\downarrow}^\dagger a_{i+y\downarrow} + H.C.] - t_b \sum_i [a_{i\uparrow}^\dagger a_{i+y\uparrow} + a_{i\downarrow}^\dagger a_{i+x\downarrow} + H.C.] \\
& + J \sum_i [(a_{i\uparrow}^\dagger a_{i+x\downarrow} - a_{i\downarrow}^\dagger a_{i+x\uparrow}) - i(a_{i\uparrow}^\dagger a_{i+y\downarrow} + a_{i\downarrow}^\dagger a_{i+y\uparrow}) + H.C.] \\
& - \sum_{i\sigma} (\mu + \sigma\Gamma) a_{i\sigma}^\dagger a_{i\sigma} - \Delta \sum_i (a_{i\uparrow}^\dagger a_{i\downarrow}^\dagger + H.C.)
\end{aligned} \tag{10}$$

where $a_{i\sigma}^\dagger$ is the creation operator of a fermion with spin σ at lattice site $i = (i_x, i_y)$. Without loss of generality we suppose that the system has two open boundary in the x -direction and is periodic in the y -direction. After performing a Fourier transformation along the y -direction only, we numerically diagonalize the Hamiltonian (10) and correspondingly obtain the excitation spectrum E_{n,k_y} with subscript n labeling different energy levels.

In Fig.2 we shows the energy spectra for an ASIOL with edges at $i_x = 0$ and $i_x = 30$. These 12 figures correspond to 12 regions in Fig.1(a), respectively. Fig.2(b), (d), (f), (h), (j) are for non-Abelian TS phases, (k) for Abelian TS phase and others non-TS phases. As stated in [30, 33], we also find that in the non-Abelian TS phases, where $I_{TKNN} = \pm 1$ and $(-1)^{I_{TKNN}} = -1$, a single pair of gapless edge modes appears. Since on a given boundary there is no state available for backward spinconserving scattering, these states are topologically protected [33]. In this case the edge zero mode is a chiral Majorana fermion. While in Abelian TS phase $I_{TKNN} = 2$ and non-TS phases $I_{TKNN} = 0$, where $(-1)^{I_{TKNN}} = 1$, the system contains either zero or two pairs of edge states. These edge states are topologically trivial for either edge modes can perform spin-conserving backscattering. In addition it is also found that edge excitations only cross at zero energy with a linear dispersion at $k_y = 0$ or π . Their origin is topological and can be identified by a topological winding number $I(k_y)$ defined only for $k_y = 0$ and π [30]: when $I(k_y)$ is non-zero for $k_y = 0$ or π , the energy of the gapless edge mode becomes zero at this value of k_y .

3 Phase Diagram with Self-Consistent Pairing Gap

In section 2 we have determined the topological phase diagram for a fixed s-wave superfluid pairing gap. However for a realistic physical system the pairing gap generally varies when the chemical potential and Zeeman magnetic field change. Especially Zeeman magnetic field breaks time-reversal symmetry and weakens the stability of superfluidity. A well-known example is so-called Chandrasekar-Clogston (CC) limit [34, 35] in superconducting systems

without SOC. Hence it is possible that not all phases in Fig.1(a) are accessible. In this section within BCS mean-field theory, we self-consistently determine s-wave superfluid pairing gap and consider the competition from normal phase and phase separation to investigate the stability of TS.

Let $-U$ ($U > 0$) denote the effective attraction strength between fermions, then the pairing gap $\Delta = U \sum_k \langle a_{-k\downarrow} a_{k\uparrow} \rangle$ can be obtained from the minimization of thermodynamic potential $\Omega_s = \sum_k \left[\xi_{k+} - \frac{1}{2}(E_k^+ + E_k^-) \right] + N\Delta^2/U$. The instability of superfluidity against phase separation is signalled by the condition $\Delta \neq 0$ and $\partial^2\Omega_s/\partial\Delta^2 < 0$, while instability against normal state is $\Omega_n < \Omega_s$, where Ω_n is thermodynamic potential of normal state. For parameter chosen superfluidity is robust as long as $\Delta \neq 0$. The resulting zero-temperature pairing gap and phase diagram are shown in Fig.3. Fig.3(b) shows similar structures with Fig.1(a) except TS with large Zeeman magnetic field are not available. Comparing Fig.3(a) with (b), it is easily seen that for small chemical potential and Zeeman magnetic field, although the pairing gap has a larger magnitude ($\Delta \sim t_a$) than Zeeman magnetic field, the system can be non-Abelian TS with $I_{TKNN} = -1$. This finding is very important and suggests that such a new non-Abelian TS we have found in section 2 is stable.

At last we consider the effects of a harmonic trap potential by local density approximation (LDA). Under this approximation the system is locally uniform and trap potential effectively provides a scan over the chemical potential, in other words local chemical potential $\mu_R = \mu - \Delta_t R^2$ with Δ_t denoting the strength of an isotropic potential. From Fig.3(b) depending on Zeeman magnetic field some different topological phases can coexist in different concentric spherical shells. In Fig.4 we show the space distributions of pairing gap, particle number and TKNN number. It should be noted that on the boundary of different topological phases there always exists zero-energy states due to the change of topological invariant.

4 Conclusions

In conclusion we have investigated the effects of an anisotropic and spin-dependent optical lattice (ASDOL) on non-Abelian topological superfluid and found that a new non-Abelian topological superfluid phase exists steadily, in contrast to an isotropic and spin-independent optical lattice. Moreover in this new non-Abelian topological superfluid phase Zeeman magnetic field can be smaller than the superfluid pairing gap. Thus an ASDOL supplies a convenient route to realize TS. In addition we also calculated chiral Majorana edge states and investigated the effects of a harmonic trap potential.

Acknowledgement

The work was supported by National Natural Science Foundation of China under Grant No. 10675108 and Foundation of Yancheng Institute of Technology under Grant No. XKR2010007.

References

- [1] E. Majorana, *Nuovo Cimento* 5, 171 (1937).
- [2] C. Nayak, S. H. Simon, A. Stern, M. Freedman and S. Das Sarma, *Rev. Mod. Phys.* 80, 1083 (2008).
- [3] X.-L. Qi and S.-C. Zhang, *Rev. Mod. Phys.* 83, 1057 (2011).
- [4] M. Z. Hasan and C. L. Kane, *Rev. Mod. Phys.* 82, 3045 (2010).
- [5] N. Read and D. Green, *Phys. Rev. B* 61, 10267 (2000).
- [6] Y. Tsutsumi, T. Kawakami, T. Mizushima, M. Ichioka and K. Machida, *Phys. Rev. Lett.* 101, 135302 (2008).
- [7] M. Sato and S. Fujimoto, *Phys. Rev. B* 79, 094504 (2009).
- [8] P. A. Lee, arXiv:0907.2681.
- [9] L. Fu and C. L. Kane, *Phys. Rev. Lett.* 100, 096407 (2008).
- [10] J. Linder, Y. Tanaka, T. Yokoyama, A. Sudbo and N. Nagaosa, *Phys. Rev. Lett.* 104, 067001 (2010).
- [11] J. D. Sau, R. M. Lutchyn, S. Tewari, and S. Das Sarma, *Phys. Rev. Lett.* 104, 040502 (2010).
- [12] J. Alicea, *Phys. Rev. B* 81, 125318 (2010).
- [13] V. Gurarie, L. Radzihovsky and A. V. Andreev, *Phys. Rev. Lett.* 94, 230403 (2005).
- [14] C. Zhang, S. Tewari, R.M. Lutchyn and S. Das Sarma, *Phys. Rev. Lett.* 101, 160401 (2008).
- [15] P. Wang, Z. Yu, Z. Fu, J. Miao, L. Huang, S. Chai, H. Zhai and J. Zhang, arXiv:1204.1887.
- [16] L. W. Cheuk, A. T. Sommer, Z. Hadzibabic, T. Yefsah, W. S. Bakr and M. W. Zwierlein, arXiv:1205.3483.
- [17] M. Sato, Y. Takahashi and S. Fujimoto, *Phys. Rev. Lett.* 103, 020401 (2009).
- [18] O. Mandel, M. Greiner, A. Widera, T. Rom, T. W. Hänsch and I. Bloch, *Nature(London)* 425, 937 (2003).
- [19] O. Mandel, M. Greiner, A. Widera, T. Rom, T. W. Hänsch and I. Bloch, *Phys. Rev. Lett.* 91, 010407 (2003).
- [20] W. V. Liu, F. Wilczek and P. Zoller, *Phys. Rev. A* 70, 033603 (2004).
- [21] D. Jaksch and P. Zoller, *Ann. Phys.* 315, 52 (2005).

- [22] D. J. Thouless, M. Kohmoto, M. P. Nightingale and M. Nijs, Phys. Rev. Lett. 49, 405 (1982).
- [23] A. E. Feiguin and M. P. A. Fisher, Phys. Rev. Lett. 103, 025303 (2009).
- [24] G. Sarma, J. Phys. Chem. Solids 24, 1029 (1963).
- [25] W. V. Liu and F. Wilczek, Phys. Rev. Lett. 90, 047002 (2003).
- [26] M. M. Forbes, E. Gubankova, W. V. Liu and F. Wilczek, Phys. Rev. Lett. 94, 017001 (2005).
- [27] Z. Cai, L. Wang, J. Li, S. Chen, X. C. Xie and Y. Wang, arXiv:0910.0508.
- [28] L. M. Wong and K. T. Law, arXiv:1110.4575.
- [29] A. P. Schnyder, S. Ryu, A. Furusaki and A. W. W. Ludwig, Phys. Rev. B 78, 195125 (2008)
- [30] M. Sato, Y. Takahashi and S. Fujimoto, Phys. Rev. B 82, 134521 (2010).
- [31] T. Fukui, Y. Hatsugai and H. Suzuki, J. Phys. Soc. Jpn. 74, 1674 (2005).
- [32] N. Goldman, I. Satija, P. Nikolic, A. Bermudez, M. A. Martin-Delgado, M. Lewenstein and I. B. Spielman, Phys. Rev. Lett. 105, 255302 (2010).
- [33] A. Kubasiak, P. Massignan and M. Lewenstein, Europhys. Lett. 92, 46004 (2010).
- [34] A. M. Clogston, Phys. Rev. Lett. 9, 226 (1962).
- [35] B. S. Chandrasekhar, Appl. Phys. Lett. 1, 7 (1962).

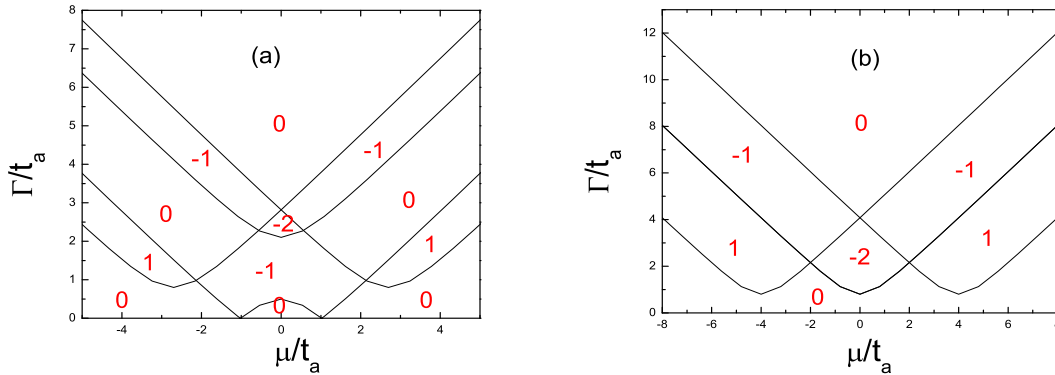


Figure 1: Topological phase diagram. The numbers in different regions are TKNN numbers. We have chosen $t_b/t_a = 0.35$, $J/t_a = 0.5$ and $\Delta/t_a = 0.8$. (a) is for an anisotropic and spin-dependent optical lattice and (b) is for an isotropic and spin-independent optical lattice.

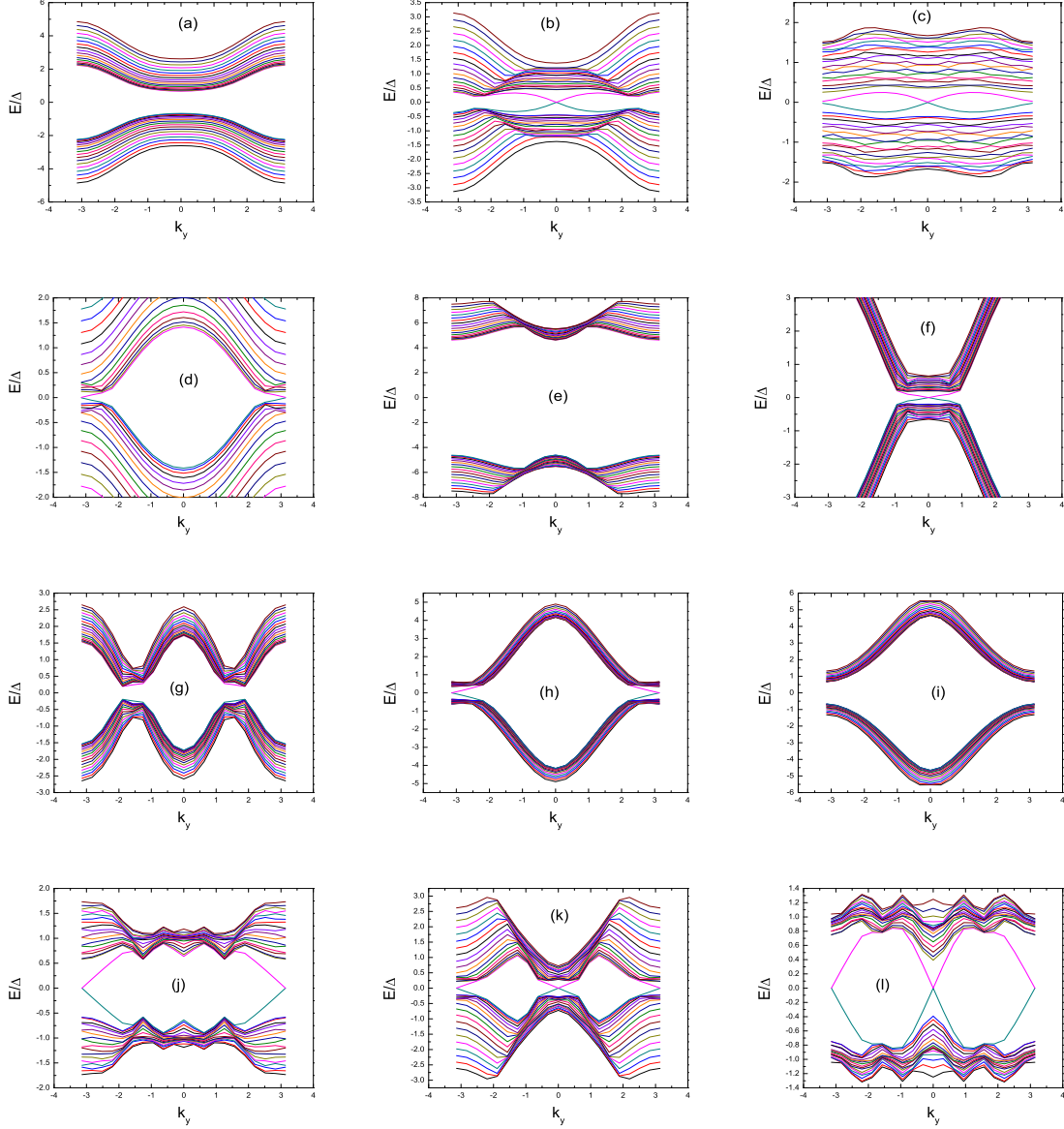


Figure 2: The energy spectra of an anisotropic and spin-dependent optical lattice with open edges at $i_x = 0$ and $i_x = 30$. We have chosen $t_b/t_a = 0.35$, $J/t_a = 0.5$ and $\Delta/t_a = 0.8$. (a) $\mu/t_a = -4.0$, $\Gamma/t_a = 1.0$, (b) $\mu/t_a = -4.0$, $\Gamma/t_a = 2.5$, (c) $\mu/t_a = -4.0$, $\Gamma/t_a = 4.0$, (d) $\mu/t_a = -4.0$, $\Gamma/t_a = 6.5$, (e) $\mu/t_a = 0.0$, $\Gamma/t_a = 6.5$, (f) $\mu/t_a = 4.0$, $\Gamma/t_a = 6.0$, (g) $\mu/t_a = 4.0$, $\Gamma/t_a = 4.0$, (h) $\mu/t_a = 4.0$, $\Gamma/t_a = 2.0$, (i) $\mu/t_a = 4.0$, $\Gamma/t_a = 1.0$, (j) $\mu/t_a = 0.0$, $\Gamma/t_a = 1.0$, (k) $\mu/t_a = 0.0$, $\Gamma/t_a = 2.5$, (l) $\mu/t_a = 0.0$, $\Gamma/t_a = 0.2$. These figures correspond to different regions in Fig.1(a), respectively.

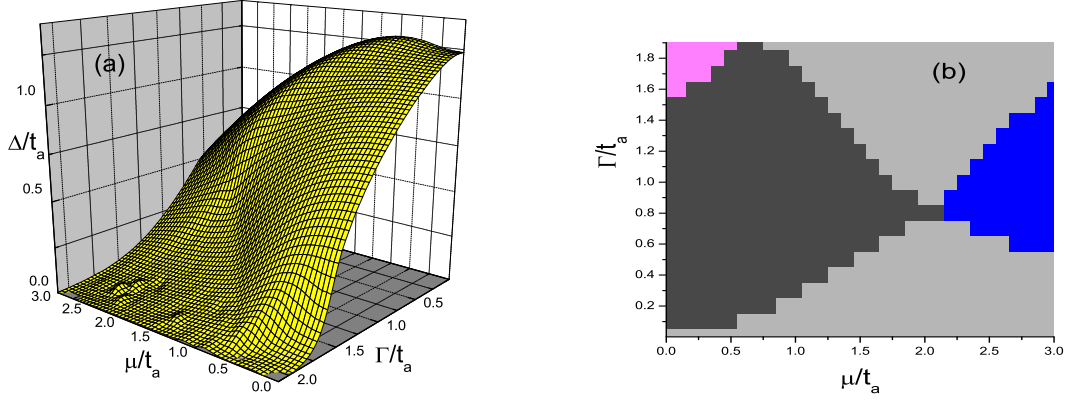


Figure 3: s-wave superfluid pairing gap (a) and topological phase diagram (b) from self-consistent mean-field solution. In (b) grey, black, blue and purple colors correspond to $I_{TKNN} = 0, -1, 1, -2$ respectively. We have chosen $t_b/t_a = 0.35$, $J/t_a = 0.5$ and $U/t_a = 4.0$.

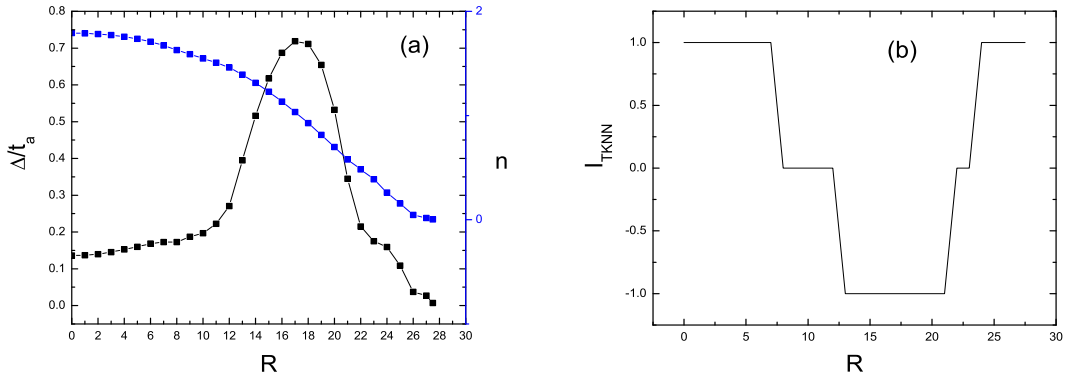


Figure 4: The space distributions of pairing gap, particle number and TKNN number. We have chosen $t_b/t_a = 0.35$, $J/t_a = 0.5$, $\mu/t_a = 3$, $\Delta_t/t_a = 0.01$, $\Gamma/t_a = 1.2$ and $U/t_a = 4.0$.